Modern Physics Letters B
Vol. 39, No. 23 (2025) 2550088 (21 pages)

DOI: 10.1142/S0217984925500885

Multiple soliton and singular wave solutions with bifurcation analysis for a strain wave equation arising in microcrystalline materials

Dean Chou

Department of Biomedical Engineering, National Cheng Kung University, Tainan 701401, Taiwan

Miin Wu School of Computing, National Cheng Kung University, Tainan 701401, Taiwan

Salah Mahmoud Boulaaras

Department of Mathematics, College of Science, Qassim University, Buraydah 51452, Saudi Arabia

Hamood Ur Rehman* and Ifrah Iqbal

Department of Mathematics, University of Okara, Okara, Pakistan
**hamood84@gmail.com*

Wen-Xiu Ma†

Department of Mathematics, Zhejiang Normal University, Jinhua 321004, China

Department of Mathematics, King Abdulaziz University, Jeddah 21589, Saudi Arabia

Department of Mathematics and Statistics, University of South Florida, Tampa, FL 33620-5700, USA

Material Science Innovation and Modelling, Department of Mathematical Sciences, North-West University, Mafikeng Campus, Mmabatho 2735, South Africa
mawx@cas.usf.edu

Received 9 July 2024
Revised 4 September 2024
Accepted 30 September 2024
Published 23 December 2024

A microcrystalline material refers to a crystallized substance or rock comprised of tiny crystals that can only be observed under a microscope. The strain wave equation is a fourth-order nonlinear partial differential equation encountered in the examination of non-dissipative strain wave propagation within microstructured solids. In this paper, the transmission of waves in

†Corresponding author.

microcrystalline materials is dictated by the non-dissipative case of strain wave equation's structure, accounting for multiple dimensions within microcrystalline structures. The simplest equation method is employed to extract multi-soliton solutions, while the modified Sardar subequation method is applied to identify additional soliton solutions, including bright, combined dark–bright, combined dark-singular, periodic singular, and singular solitons. Furthermore, the dynamical system bifurcation theory approach is utilized to investigate the phase diagrams of the governing equation. Further elaboration on the physical dynamical representation of the presented solutions is provided through profile illustrations. A comparison with the existing literature is also provided, highlighting the efficacy of our work. The significance of the acquired outcomes lies in their capacity to portray a wide array of intricate and diverse phenomena observed in both mathematical and physical systems.

Keywords: Strain wave equation; multi-solitons; phase portrait; microcrystalline materials; nonlinear equations.

PACS Nos.: 02.30.Ik, 05.45.Yv

1. Introduction

Nonlinear phenomena are prevalent across different fields in engineering and applied sciences, serving as fundamental models for both natural and social occurrences. A myriad of nonlinear evolution equations (NLEEs) has been formulated to explain these intricate nonlinear dynamics including plasma hydrodynamics, chemical dynamics, population modeling and solid-state physics.[1–5] The solutions obtained from NLEEs are significant in nonlinear science because they offer crucial insights into the underlying physical properties of the phenomena under investigation. These investigations not only enhance our comprehension of the problem's properties, but also furnish valuable predication for future practical applications.[6–10] Researchers extract different types of soliton solutions of NLEEs such as lump wave solutions of $(2+1)$-dimensional dispersive wave model,[11] N-soliton solutions of nonlinear integrable equations are obtained by the Hirota bilinear method,[12] N-soliton solutions of nonlinear integrable equations involving reflection points of coordinates are generated in detail by Darboux transformations,[13] and solutions derived from the Riemann–Hilbert problems.[14]

NLEEs also serve as mathematical models for explaining wave propagation in microstructured solids.[15,16] The consideration of multiple microcrystalline solids becomes imperative, particularly when scale dependence introduces nonlinear behavior and dispersion effects. In such cases, the relation between dispersion and nonlinear effects can lead to the occurrence of solitary waves. Microcrystalline solids have crystal domains on the micrometer scale which is the characteristic of these materials. The microcrystalline solids may be affected by different factors, such as existence of grain boundaries and grain size[17,18] which have potential to impede dislocation movement. Moreover, the electrical conductivity of microcrystalline materials is different from that of both single crystals and amorphous materials. Grain boundaries can also effect on charge carrier mobility which add further complexity to their electrical behavior. Microcrystalline solids, such as silicon, have size-dependent optical properties and are key components in semiconductor devices and thin-film solar cells.[19,20] Their controlled microstructure enables cost-effective

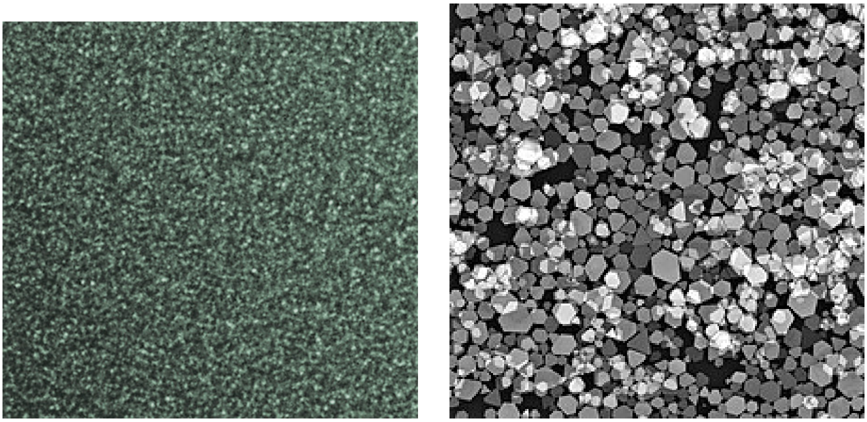

(a) Silicon Microcrystalline

(b) Silver Microcrystalline

Fig. 1. (Color online) Images of microcrystalline materials.[25,26]

production processes while maintaining efficiency to make them valuable in the manufacturing of electronic component. Additionally, other metallic alloys with microcrystalline structures influence mechanical properties and are crucial for components requiring specific strength and toughness. Microcrystalline materials also find applications in MEMS devices, where their tailored mechanical and electrical properties are leveraged in emerging technologies.[21,22] The images of microcrystalline materials are illustrated in Fig. 1.

The strain wave equation, a fourth-order nonlinear partial differential equation, emerges as a fundamental tool in analyzing non-dissipative strain wave propagation within microstructured solids.[23] Beyond its application in this context, it serves as a versatile model capturing the dynamics of various physical phenomena. Additionally, it can be viewed as an extension of the Boussinesq equation, incorporating dual dispersion effects. The equation's scope encompasses phenomena such as shallow water waves in oceanic regions, nonlinear lattice waves, and vibrations of nonlinear strings.[24] Strain, a fundamental measure of material deformation, quantifies either the stretch or compression (normal strains) or the distortion associated with inter-layer sliding (shear strains) within a material. Strain measurement stands as a cornerstone in materials testing, offering insights into the physical properties of materials through stress–strain curves. Engineers leverage this knowledge to compare materials and predict the behavior of structures or components made from specific materials, accounting for factors like stiffness and failure strength during processing and service.

Within microcrystalline solids, the strain wave equation takes on the following form[27,28]:

$$Y_{tt} - Y_{xx} - a(l_1(Y^2)_{xx} - \epsilon l_2 Y_{xxt} + \chi l_3 Y_{xxxx} - (\chi l_4 - \epsilon^2 l_7)Y_{xxtt} + \epsilon\chi(Y_{xxxxtt} + l_6 Y_{xxxttt}) = 0, \tag{1}$$

where $l_i (i = 1, 2, \ldots, 7)$ are nonzero real numbers, a signifies the influence of dissipation, ϵ represents the coefficient associated with elastic strain, and χ denotes the ratio between the size and wavelength of the microstructure. By putting $\epsilon = 0$ and $\chi = O(\epsilon)$, the (1) turns into the following equation[29]

$$Y_{tt} - Y_{xx} - a(l_1(Y^2)_{xx} - l_3 Y_{xxxx} + l_4 Y_{xxtt}) = 0. \tag{2}$$

Recent studies have focused extensively on the strain wave dynamical equation, yielding a variety of solutions such as in Ref. 30, authors examined the strain wave equation and derived several traveling wave solutions using a novel generalized G'/G- expansion method. In Ref. 31, strain wave equation is explored to uncover various soliton solutions through extended simple equation. In Ref. 27, the explicit solutions for the strain wave model are obtained by utilizing the effective functional variable techniques and Kudryashov method. In Ref. 16, authors applied a newly modified extended mapping method to the strain wave dynamical equation in microstructured solids, producing several explicit wave solutions.

As soliton theory advances, a multitude of robust methodologies have surfaced, each designed to elucidate precise solutions to NLPDEs.[32–41] There is a general approach to solitary wave solutions, called the transformed rational function method[42] and more generally, the multiple exp-function method for generating multi-wave solutions.[43]

In this paper, we explore the non-dissipative strain wave equation within microcrystalline materials, focusing specifically on (2). This problem is significant due to its implications for understanding wave propagation in microstructured solids. To address this, we employ the simplest equation method (SEM)[44] and modified Sardar subequation method (MSSEM)[45] to extract multi-soliton and other types of solutions for the first time.

The examination of differential equations (DEs) through bifurcation theory has emerged as a highly regarded area of study in recent times. These disciplines serve as valuable resources for understanding complex systems governed by DEs.[46] Bifurcation, characterized by a qualitative shift in the behavior of a dynamical system due to parameter variations, is a pivotal concept within this framework. Notably, this study marks the first investigation into bifurcation analysis within this context.

In summary, we investigate the non-dissipative strain wave equation in terms of microcrystalline materials by employing several analytical methods such as the SEM and the MSSEM, to derive various soliton solutions such as multi-solitons, bright, dark–bright, dark-singular, periodic singular, and singular solitons. Additionally, we utilized the dynamical system bifurcation theory to analyze phase diagrams to provide deeper insights into the dynamical behavior of the solutions. The results indicate the diverse wave phenomena that can occur in microcrystalline materials and contribute to a broader understanding of such systems. The novelty of this work lies in the application of advanced soliton solution techniques which extends beyond previous efforts by offering new perspectives in existing literature.

The subsequent structure of the paper unfolds as follows. Section 2 delves into the SEM with its corresponding applications. Following that, Sec. 3 provides an exposition on the MSSM, accompanied by illustrative applications. In Sec. 4, bifurcation analysis on the governed equation is thoroughly elucidated. Moving forward, Sec. 5 presents the Results and Discussion, while the final section offers the Conclusion.

2. Simplest Equation Method

The Simplest Equation Method (SEM) employs a basic reference equation, typically the Burger equation, to derive multi-soliton solutions. This approach bypasses the need for bilinearization, streamlining the process of obtaining soliton solutions. By using the Burger equation as a simplifying reference, the SEM efficiently generates solutions without resorting to complex transformations or lengthy ansatzes. This method's straightforward application allows for a more efficient and accessible analysis of the soliton structures in many nonlinear systems.

Consider the nonlinear partial differential equation (NLPDE)

$$Q(Y_t, Y_{tx}, Y_{xx}, \ldots). \tag{3}$$

Now, suppose

$$Y(x,t) = Q(\zeta), \quad \zeta = kx - ct, \tag{4}$$

where k and c denote the wave number and the wave speed, respectively. The transformation given in (4) changes the (3) into the following ordinary differential equation (ODE):

$$R\Big(Q(\zeta), \frac{dQ}{d\zeta}, \frac{dQ^2}{d\zeta^2}, \ldots\Big). \tag{5}$$

Assume that the solution of Eq. (5) is written as

$$Q(\zeta) = \sum_{j=0}^{N} g_j (V(\zeta))^j. \tag{6}$$

The process begins by expressing the constants g_j and the solution V of specific ODEs, referred to as the SE, where V is a solution of specific ODEs. Using the homogeneous balancing rule, we determine the constant N. Next, we substitute the finite-series solution given by Eq. (6) into Eq. (5), resulting in a polynomial involving V. Setting all coefficients of this polynomial to zero generates a system of equations. Solving this system allows us to determine the values of g_j. The crucial step in employing the SEM is selecting the appropriate SE. Thus, we opt for the coupled Burgers' equation, as it represents the simplest equation for discovering new solitary and multi-soliton solutions.

Consider the Burgers' equation

$$v_t - 2vv_x - v_{xx} = 0. \tag{7}$$

Now, suppose $v(x,t) = V(\zeta)$.

$$-cV_\zeta - 2kVV_\zeta - k^2 V_{\zeta\zeta} = 0. \tag{8}$$

By taking integration of (8) with respect to ζ

$$V_\xi = \frac{-c}{k^2} V - \frac{1}{k} V^2. \tag{9}$$

The dispersion relation gives

$$c = -k^2. \tag{10}$$

Hence, (9) changes to

$$V_\zeta = V - \frac{1}{k} V^2. \tag{11}$$

A general class of solutions to the Riccati equation in Ref. 47 was presented. A multi-wave solution for the Burgers' equation (7) derived using Hirota's method is written as[44]

$$V = \frac{\sum_{j=1}^{N} k_j e^{k_j x - c_j t}}{1 + \sum_{j=1}^{N} e^{k_j x - c_j t}}, \tag{12}$$

where $c_i^2 = -k_i^2$. Now by putting (9) into (6), solution of given equation is obtained.

2.1. *Application of SEM*

The (4) changes the (3) into the following ODE

$$ak^2(k^2 l_3 - c^2 l_4) Q''(\zeta) - ak^2 l_1 Q(\zeta)^2 + (c^2 - k^2) Q(\zeta) = 0. \tag{13}$$

The homogeneous balancing rule gives $N = 2$, so from (6), assume

$$Q(\zeta) = g_2 V(\zeta)^2 + g_1 V(\zeta) + g_0. \tag{14}$$

By inserting (14) along (11), we get the following set of algebraic system:

$$\begin{aligned}
g_0(c^2 - k^2) - a g_0^2 k^2 l_1 = 0, \\
a g_1 k^2 (k^2 l_3 - c^2 l_4) - 2a g_0 g_1 k^2 l_1 + g_1 (c^2 - k^2) = 0, \\
(6a g_2 (k^2 l_3 - c^2 l_4) - a g_2^2 k^2 l_1) = 0, \\
-10 a g_2 k (k^2 l_3 - c^2 l_4) + 2a g_1 (k^2 l_3 - c^2 l_4) - 2a g_1 g_2 k^2 l_1 = 0, \\
4a g_2 k^2 (k^2 l_3 - c^2 l_4) - 3a g_1 k (k^2 l_3 - c^2 l_4) - a g_1^2 k^2 l_1 - 2a g_0 g_2 k^2 l_1 + g_2 (c^2 - k^2) = 0.
\end{aligned}$$

Now, by solving this system, we have the following values of constants:

$$\begin{aligned}
& g_0 = 0, \quad g_1 = -k g_2, \quad a = \frac{k^2 - c^2}{k^2 (k^2 l_3 - c^2 l_4)}, \\
& l_1 = \frac{6(k^2 l_3 - c^2 l_4)}{g_2 k^2}.
\end{aligned}$$

When substituting the values into Eq. (14) and inserting Eq. (12) within Eqs. (6) and (4), we derive the subsequent solutions of (2)

1-soliton solution

$$Y_{1-s}(x,t) = g_2\left(\frac{k_1^2 e^{2(-c_1t+k_1x)}}{(e^{(-c_1t+k_1x)}+1)^2} - \frac{k_1^2 e^{(-c_1t+k_1x)}}{e^{(-c_1t+k_1x)}+1}\right), \tag{15}$$

where $k_1 = k$ and $c_1 = c$.

2-soliton solution

$$Y_{2-s}(x,t) = g_2\left(\frac{k_1^2 e^{2(-c_1t+k_1x)} + k_2^2 e^{2(-c_2t+k_2x)}}{(e^{(-c_1t+k_1x)}+e^{(-c_2t+k_2x)}+1)^2} - \frac{k_1^2 e^{(-c_1t+k_1x)} + k_2^2 e^{(-c_2t+k_2x)}}{e^{(-c_1t+k_1x)}+e^{(-c_2t+k_2x)}+1}\right). \tag{16}$$

3-soliton solution

$$\begin{aligned} Y_{3-s}(x,t) = g_2\Bigg(&\frac{k_1^2 e^{2(-c_1t+k_1x)} + k_2^2 e^{2(-c_2t+k_2x)} + k_3^2 e^{2(-c_3t+k_3x)}}{(e^{(-c_1t+k_1x)}+e^{(-c_2t+k_2x)}+e^{(-c_3t+k_3x)}+1)^2} \\ &- \frac{k_1^2 e^{(-c_1t+k_1x)} + k_2^2 e^{(-c_2t+k_2x)} + k_3^2 e^{(-c_3t+k_3x)}}{e^{(-c_1t+k_1x)}+e^{(-c_2t+k_2x)}+e^{(-c_3t+k_3x)}+1}\Bigg). \end{aligned} \tag{17}$$

3. Description of MSSEM

The modified Sardar Subequation method is an enhanced version of the original Sardar Subequation Method (SSM).[23] This method is employed to extract various types of solutions and has been widely applied in the literature due to its effectiveness in solving NLPDEs.

Suppose, in (6), $V(\zeta)$ satisfies the following ODE

$$V'(\zeta) = \sqrt{sV^4(\zeta) + rV^2(\zeta) + q}, \tag{18}$$

where q, r, and s are constants.

Case 1: If $q = 0$, $r > 0$, and $s \neq 0$, then

$$V_1(\zeta) = \pm\sqrt{-\frac{r}{s}}\operatorname{sech}(\sqrt{r}(\zeta+\nu)),$$
$$V_2(\zeta) = \pm\sqrt{\frac{r}{s}}\operatorname{csch}(\sqrt{r}(\zeta+\nu)).$$

Case 2: For constants δ_1 and δ_2. Let $s = \pm 4\delta_1\delta_2$, $r > 0$, and $q = 0$, we have

$$V_3(\zeta) = \pm\frac{4\delta_1\sqrt{r}}{(4\delta_1^2 - s)\cosh(\sqrt{r}(\zeta+\zeta_0)) \pm (4\delta_1^2 + s)\sinh(\sqrt{r}(\zeta+\zeta_0))}.$$

Case 3: If $q = \frac{r^2}{4s}$, $r < 0$, and $s > 0$, with constants D_1, and D_2, then

$$
\begin{aligned}
V_4(\zeta) &= \pm\sqrt{-\frac{r}{2s}}\tanh\left(\sqrt{-\frac{r}{2}}(\zeta+\nu)\right),\\
V_5(\zeta) &= \pm\sqrt{-\frac{r}{2s}}\coth\left(\sqrt{-\frac{r}{2}}(\zeta+\nu)\right),\\
V_6(\zeta) &= \pm\sqrt{-\frac{r}{2s}}(\tanh(\sqrt{-2r}(\zeta+\nu)) \pm i\operatorname{sech}(\sqrt{-2r}(\zeta+\nu))),\\
V_7(\zeta) &= \pm\sqrt{-\frac{r}{8s}}\left(\tanh\left(\sqrt{-\frac{r}{8}}(\zeta+\nu)\right) + \coth\left(\sqrt{-\frac{r}{8}}(\zeta+\nu)\right)\right),\\
V_8(\zeta) &= \pm\sqrt{-\frac{r}{2s}}\left(\frac{\pm\sqrt{D_1^2+D_2^2} - D_1\cosh(\sqrt{-2r}(\zeta+\nu))}{D_1\sinh(\sqrt{-2r}(\zeta+\nu)) + D_2}\right),\\
V_9(\zeta) &= \pm\sqrt{-\frac{r}{2s}}\left(\frac{\cosh(\sqrt{-2r}(\zeta+\nu))}{\sinh(\sqrt{-2r}(\zeta+\nu)) \pm i}\right).
\end{aligned}
$$

Case 4: If $q = 0$, $r < 0$, and $s \neq 0$, then

$$
\begin{aligned}
V_{10}(\zeta) &= \pm\sqrt{-\frac{r}{s}}\sec(\sqrt{-r}(\zeta+\nu)),\\
V_{11}(\zeta) &= \pm\sqrt{-\frac{r}{s}}\csc(\sqrt{-r}(\zeta+\nu)).
\end{aligned}
$$

Case 5: If $q = \frac{r^2}{4s}$, $r > 0$, $s > 0$, and $D_1^2 - D_2^2 > 0$, then

$$
\begin{aligned}
V_{12}(\zeta) &= \pm\sqrt{\frac{r}{2s}}\tan\left(\sqrt{\frac{r}{2}}(\zeta+\nu)\right),\\
V_{13}(\zeta) &= \pm\sqrt{\frac{r}{2s}}\cot\left(\sqrt{\frac{r}{2}}(\zeta+\nu)\right),\\
V_{14}(\zeta) &= \pm\sqrt{\frac{r}{2s}}(\tan(\sqrt{2r}(\zeta+\nu)) \pm \sec(\sqrt{2r}(\zeta+\nu))),\\
V_{15}(\zeta) &= \pm\sqrt{\frac{r}{8s}}\left(\tan\left(\sqrt{\frac{r}{8}}(\zeta+\nu)\right) - \cot\left(\sqrt{\frac{r}{8}}(\zeta+\nu)\right)\right),\\
V_{16}(\zeta) &= \pm\sqrt{\frac{r}{2s}}\left(\frac{\pm\sqrt{D_1^2-D_2^2} - D_1\cos(\sqrt{2r}(\zeta+\nu))}{D_1\sin(\sqrt{2r}(\zeta+\nu)) + D_2}\right),\\
V_{17}(\zeta) &= \pm\sqrt{\frac{r}{2s}}\left(\frac{\cos(\sqrt{2r}(\zeta+\nu))}{\sin(\sqrt{2r}(\zeta+\nu)) \pm 1}\right).
\end{aligned}
$$

Case 6: If $q = 0$ and $r > 0$, then

$$
\begin{aligned}
V_{18}(\zeta) &= \frac{4re^{\pm\sqrt{r}(\zeta+\nu)}}{e^{\pm 2\sqrt{r}(\zeta+\nu)} - 4rs},\\
V_{19}(\zeta) &= \frac{\pm 4re^{\pm\sqrt{r}(\zeta+\nu)}}{1 - 4rse^{\pm 2\sqrt{r}(\zeta+\nu)}}.
\end{aligned}
$$

Case 7: If $q = r = 0$ and $s > 0$, then

$$V_{20}(\zeta) = \pm \frac{1}{\sqrt{s}(\zeta + \nu)}.$$

Case 8: If $q = r = 0$ and $s < 0$, then

$$V_{21}(\zeta) = \pm \frac{i}{\sqrt{-s}(\zeta + \nu)}.$$

Putting (18) along (6) into (13) and equating all the coefficients to zero yield a system that can be solved to find g_j.

3.1. *Application of MSSEM*

The homogeneous balancing rule gives $N = 2$, so from (6), assume

$$Q(\zeta) = g_2 V(\zeta)^2 + g_1 V(\zeta) + g_0. \tag{19}$$

By inserting (19) with (18) into (13), we get the following set of algebraic system:

$$\begin{aligned}
&-2ac^2 g_2 k^2 l_4 q + 2ag_2 k^4 l_3 q - ag_0^2 k^2 l_1 + c^2 g_0 - g_0 k^2 = 0,\\
&-ac^2 g_1 k^2 l_4 r + ag_1 k^4 l_3 r - 2ag_0 g_1 k^2 l_1 + c^2 g_1 - g_1 k^2 = 0,\\
&-2ac^2 g_1 k^2 l_4 s + 2ag_1 k^4 l_3 s - 2ag_1 g_2 k^2 l_1 = 0,\\
&-4ac^2 g_2 k^2 l_4 r + 4ag_2 k^4 l_3 r - ag_1^2 k^2 l_1 - 2ag_0 g_2 k^2 l_1 + c^2 g_2 - g_2 k^2 = 0,\\
&-6ac^2 g_2 k^2 l_4 s + 6ag_2 k^4 l_3 s - ag_2^2 k^2 l_1 = 0.
\end{aligned}$$

The following sets of constants are obtained by solving the above system

Set 1:

$$\begin{aligned}
r &= \frac{\sqrt{c^4 - 2c^2k^2 + k^4}}{4(ac^2k^2l_4 - ak^4l_3)}, \quad g_1 = 0, \quad g_2 = -\frac{6(c^2 l_4 s - k^2 l_3 s)}{l_1},\\
g_0 &= \frac{c^2 l_1 - l_1\sqrt{c^4 - 2c^2k^2 + k^4} - k^2 l_1}{2ak^2 l_1^2}.
\end{aligned}$$

Set 2:

$$g_1 = 0, \quad g_0 = \frac{k^2 - c^2}{2ak^2 l_1}, \quad l_4 = \frac{2ak^4 l_3 r + c^2 - k^2}{2ac^2k^2 r}, \quad s = -\frac{ag_2 k^2 l_1 r}{3(c^2 - k^2)}.$$

Now, by using the values of constants in (19) and by using the solutions of (13), we have the following solutions of governed equation. The solutions of Case 3 and Case 5 are according to Set 2 and remaining cases are according to Set 1.

Case 1: If $q = 0$, $r > 0$, and $s \neq 0$, then

$$Y_1(\zeta) = g_0 + g_2\left(\pm\sqrt{-\frac{r}{s}}\operatorname{sech}(\sqrt{r}(\zeta + \nu))\right)^2, \tag{20}$$

$$Y_2(\zeta) = g_0 + g_2\left(\pm\sqrt{\frac{r}{s}}\mathrm{csch}(\sqrt{r}(\zeta+\nu))\right)^2. \tag{21}$$

Case 2: For constants δ_1 and δ_2. Let $s = \pm 4\delta_1\delta_2$, $r > 0$, and $q = 0$, we have

$$Y_3(\zeta) = g_0 + g_2\left(\pm\frac{4\delta_1\sqrt{r}}{(4\delta_1^2 - s)\cosh(\sqrt{r}(\zeta+\zeta_0)) \pm (4\delta_1^2 + s)\sinh(\sqrt{r}(\zeta+\zeta_0))}\right)^2. \tag{22}$$

Case 3: If $q = \frac{r^2}{4s}$, $r < 0$, and $s > 0$, with constants D_1, and D_2, then

$$Y_4(\zeta) = \frac{k^2 - c^2}{2ak^2 l_1} + g_2\left(\pm\sqrt{-\frac{r}{2s}}\tanh\left(\sqrt{-\frac{r}{2}}(\zeta+\nu)\right)\right)^2, \tag{23}$$

$$Y_5(\zeta) = \frac{k^2 - c^2}{2ak^2 l_1} + g_2\left(\pm\sqrt{-\frac{r}{2s}}\coth\left(\sqrt{-\frac{r}{2}}(\zeta+\nu)\right)\right)^2, \tag{24}$$

$$Y_6(\zeta) = \frac{k^2 - c^2}{2ak^2 l_1} + g_2\left(\pm\sqrt{-\frac{r}{2s}}(\tanh(\sqrt{-2r}(\zeta+\nu)) \pm i\,\mathrm{sech}(\sqrt{-2r}(\zeta+\nu)))\right)^2, \tag{25}$$

$$Y_7(\zeta) = \frac{k^2 - c^2}{2ak^2 l_1} + g_2\left(\pm\sqrt{-\frac{r}{8s}}\left(\tanh\left(\sqrt{-\frac{r}{8}}(\zeta+\nu)\right) + \coth\left(\sqrt{-\frac{r}{8}}(\zeta+\nu)\right)\right)\right)^2, \tag{26}$$

$$Y_8(\zeta) = \frac{k^2 - c^2}{2ak^2 l_1} + g_2\left(\pm\sqrt{-\frac{r}{2s}}\left(\frac{\pm\sqrt{D_1^2 + D_2^2} - D_1\cosh(\sqrt{-2r}(\zeta+\nu))}{D_1\sinh(\sqrt{-2r}(\zeta+\nu)) + D_2}\right)\right)^2, \tag{27}$$

$$Y_9(\zeta) = \frac{k^2 - c^2}{2ak^2 l_1} + g_2\left(\pm\sqrt{-\frac{r}{2s}}\left(\frac{\cosh(\sqrt{-2r}(\zeta+\nu))}{\sinh(\sqrt{-2r}(\zeta+\nu)) \pm i}\right)\right)^2. \tag{28}$$

Case 4: If $q = 0$, $r < 0$, and $s \neq 0$, then

$$Y_{10}(\zeta) = g_0 + g_2\left(\pm\sqrt{-\frac{r}{s}}\sec(\sqrt{-r}(\zeta+\nu))\right)^2, \tag{29}$$

$$Y_{11}(\zeta) = g_0 + g_2\left(\pm\sqrt{-\frac{r}{s}}\csc(\sqrt{-r}(\zeta+\nu))\right)^2. \tag{30}$$

Case 5: If $q = \frac{r^2}{4s}$, $r > 0$, $s > 0$, and $D_1^2 - D_2^2 > 0$, then

$$Y_{12}(\zeta) = \frac{k^2 - c^2}{2ak^2 l_1} + g_2\left(\pm\sqrt{\frac{r}{2s}}\tan\left(\sqrt{\frac{r}{2}}(\zeta+\nu)\right)\right)^2, \tag{31}$$

$$Y_{13}(\zeta) = \frac{k^2 - c^2}{2ak^2 l_1} + g_2\left(\pm\sqrt{\frac{r}{2s}}\cot\left(\sqrt{\frac{r}{2}}(\zeta+\nu)\right)\right)^2, \tag{32}$$

$$Y_{14}(\zeta) = \frac{k^2 - c^2}{2ak^2 l_1} + g_2\left(\pm\sqrt{\frac{r}{2s}}(\tan(\sqrt{2r}(\zeta+\nu)) \pm \sec(\sqrt{2r}(\zeta+\nu)))\right)^2, \tag{33}$$

$$Y_{15}(\zeta) = \frac{k^2 - c^2}{2ak^2 l_1} + g_2\left(\pm\sqrt{\frac{r}{8s}}\left(\tan\left(\sqrt{\frac{r}{8}}(\zeta+\nu)\right) - \cot\left(\sqrt{\frac{r}{8}}(\zeta+\nu)\right)\right)\right)^2, \tag{34}$$

$$Y_{16}(\zeta) = \frac{k^2 - c^2}{2ak^2 l_1} + g_2\left(\pm\sqrt{\frac{r}{2s}}\left(\frac{\pm\sqrt{D_1^2 - D_2^2} - D_1\cos(\sqrt{2r}(\zeta+\nu))}{D_1\sin(\sqrt{2r}(\zeta+\nu)) + D_2}\right)\right)^2, \tag{35}$$

$$Y_{17}(\zeta) = \frac{k^2 - c^2}{2ak^2 l_1} + g_2\left(\pm\sqrt{\frac{r}{2s}}\left(\frac{\cos(\sqrt{2r}(\zeta+\nu))}{\sin(\sqrt{2r}(\zeta+\nu)) \pm 1}\right)\right)^2. \tag{36}$$

Case 6: If $q = 0$ and $r > 0$, then

$$Y_{18}(\zeta) = g_0 + g_2\left(\frac{4re^{\pm\sqrt{r}(\zeta+\nu)}}{e^{\pm 2\sqrt{r}(\zeta+\nu)} - 4rs}\right)^2, \tag{37}$$

$$Y_{19}(\zeta) = g_0 + g_2\left(\frac{\pm 4re^{\pm\sqrt{r}(\zeta+\nu)}}{1 - 4rse^{\pm 2\sqrt{r}(\zeta+\nu)}}\right)^2. \tag{38}$$

Case 7: If $q = r = 0$ and $s > 0$, then

$$Y_{20}(\zeta) = g_0 + g_2\left(\pm\frac{1}{\sqrt{s}(\zeta+\nu)}\right)^2. \tag{39}$$

Case 8: If $q = r = 0$ and $s < 0$, then

$$Y_{21}(\zeta) = g_0 + g_2\left(\pm\frac{i}{\sqrt{-s}(\zeta+\nu)}\right)^2. \tag{40}$$

4. Bifurcation Analysis

In our study, the bifurcation analysis is applied to the ODEs derived from the strain wave equation, which are transformed into a Hamiltonian system for detailed analysis. By solving this Hamiltonian system, we identify the equilibrium points that characterize the system's behavior. Our observations reveal that, by varying the values of the constants used in the ODEs, we can observe different types of equilibrium points, including center points, saddle points, and cusp points. These equilibrium points indicate the qualitative changes in the system's behavior with the selection of parameters.

The (13) can be written as

$$Q''(\zeta) = \frac{ak^2 l_1}{ak^2(k^2 l_3 - c^2 l_4)} Q(\zeta)^2 - \frac{(c^2 - k^2)}{ak^2(k^2 l_3 - c^2 l_4)} Q(\zeta). \tag{41}$$

The (41) has the following Hamiltonian system:

$$\begin{aligned} \frac{dQ}{d\zeta} &= U, \\ \frac{dU}{d\zeta} &= b_1 Q^2 - b_2 Q, \end{aligned} \tag{42}$$

having the Hamiltonian

$$H(Q, U) = \frac{1}{2} U^2 - \frac{b_1}{3} Q^3 + \frac{b_2}{2} Q^2, \tag{43}$$

where

$$b_1 = \frac{ak^2 l_1}{ak^2(k^2 l_3 - c^2 l_4)}, \quad b_2 = \frac{(c^2 - k^2)}{ak^2(k^2 l_3 - c^2 l_4)}.$$

In order to study the phase portraits of the system in (42), we first study the equilibrium points of the system (42). It is easy to see that when $b_2 \neq 0$, the system (42) has two equilibrium points $V_0(0, 0)$ and $V_1(\frac{b_2}{b_1}, 0)$. When $b_2 = 0$, the system (41) has only one equilibrium point.

Case 1: When $b_2 > 0$, the origin $V_0(0, 0)$ is center point and $V_1(\frac{b_2}{b_1}, 0)$ is a saddle point. The parameters' selection is $c = 2,\ k = 1,\ l_3 = 3,\ l_4 = 1,\ a = -1.5$, and $l_1 = \pm 1$.

Case 2: When $b_2 < 0$, the origin $V_0(0, 0)$, is saddle point and $V_1(\frac{b_2}{b_1}, 0)$ is a center point. The parameters' selection is $c = 2,\ k = 1,\ l_3 = 3,\ l_4 = 1,\ a = 1$, and $l_1 = \pm 1$.

Case 3: When $b_2 = 0$, the origin $V_0(0, 0)$ is cusp point. The parameters selection is $c = 1,\ k = 1,\ l_3 = 3,\ l_4 = 1,\ a = 1$, and $l_1 = \pm 1$.

5. Results and Discussion

In this study, we employed distinct methodologies, namely SEM and MSSM, to extract various types of soliton solutions. The SEM method facilitated the exploration of multi-soliton solutions, while the modified Sardar subequation technique was utilized to derive different types of soliton solutions, including dark, bright, combined dark–bright, combined singular-dark, periodic singular, and singular solitons. We have performed a bifurcation analysis and generated phase portrait graphs, offering a novel perspective on the dynamics of the equations under study. This aspect has not been previously explored in the literature, particularly concerning multi-soliton solutions and their phase portraits. The motivation for employing the MSSEM arises from our prior investigation, where the Sardar sub-equation method yielded only 14 solutions.[23] In contrast, applying MSSEM in this study has led to the discovery of twenty solutions. This study extends these findings by providing a more comprehensive investigation, uncovering additional solution structures and advancing the understanding of wave phenomena in microcrystalline solids.

In Table 1, we present findings that align with existing research.

The applied methods have some advantages and limitations, which are summarized in Table 2. Microcrystalline solids hold promise across diverse applications within soliton wave theory, notably in optics, photonics, and condensed matter physics. Tailored microcrystalline materials exhibiting specific nonlinear optical characteristics offer opportunities for advancing optical device technologies leveraging solitons. Nonlinearities within these materials facilitate soliton formation and stabilization, offering avenues for information transmission and processing in optical communication systems. In the realm of optics, microcrystalline structures exert a profound influence on soliton behavior within optical fibers, enhancing the design and efficacy of communication networks. Furthermore, in condensed matter physics, the presence of microcrystalline structures in semiconductors shapes soliton dynamics, impacting the behavior of charge carriers and excitons. Photonic crystals featuring microcrystalline structures interact intricately with solitons, modulating their propagation and characteristics. Such interactions serve as a foundation for developing innovative devices with tailored optical functionalities, including soliton control and manipulation. The application of soliton theory to microcrystalline materials holds potential in biomedical optics. Solitons may find utility in precise imaging techniques and the manipulation of biological structures at the microscopic level, heralding new possibilities for biomedical research and clinical applications.

Using both 3D and 2D plots, we provide numerical simulations of these figures. Figures 2–4 depict solutions extracted from SEM. Specifically, Fig. 2 illustrates the 1-soliton solution, Fig. 3 shows the 2-soliton solution, and Fig. 4 indicates the 3-soliton solution. Detailed parameter descriptions are provided beneath each figure's caption.

Figures 5–8 showcase the graphs of solutions obtained from MSSM, utilizing the parameter values specified in each figure's caption. Specifically, Fig. 5 illustrates the combined dark–bright soliton solution for $Y_6(\zeta)$ and Fig. 6 depicts the combined dark-singular soliton solution for $Y_7(\zeta)$. Combined solitons, dark-singular or such as dark–bright solitons, show complex waveforms that have characteristics of more than one soliton type simultaneously. These solitons indicate interactions between different types of waves within the material. The combined solitons gives insights about complex physical systems where multiple wave types interact, such as in advanced materials with mixed properties and multi-faceted optical systems.

Figure 7 presents the periodic-singular soliton solution for $Y_{10}(\zeta)$). These solitons have features of both singularities and periodic waves which represent the waves that periodically reach infinite amplitude. In microcrystalline materials, these solutions

Table 1. Comparison between our solutions and Rehman *et al.*[23]

Our solutions	Solutions from Rehman *et al.*[23]
If $Y_1(\zeta) = I_1(\zeta), s = 1, \nu = 0$, then $I_1(\zeta) = g_0 + g_2(\pm\sqrt{-r}\mathrm{sech}(\sqrt{r}(\zeta)))^2$.	If $g_0 = \frac{-A^2+(B^2\pm(A^2-B^2)}{2A^2r_1\epsilon}, g_2 = \frac{6A^2r_3-B^2r_4}{r_1}, r = \pm\frac{A^2-B^2}{4(A^4r_3-A^2B^2r_4)}, pq = 1$, then solution (12) becomes $I_1(\zeta) = g_0 + g_2(\pm\sqrt{-r}\mathrm{sech}(\sqrt{r}(\zeta)))^2$.
If $Y_2(\zeta) = I_2(\zeta), s = 1, \nu = 0$, then $I_2(\zeta) = g_0 + g_2(\pm\sqrt{r}\mathrm{csch}(\sqrt{r}(\zeta)))^2$.	If $g_0 = \frac{-A^2+(B^2\pm(A^2-B^2)}{2A^2r_1\epsilon}, g_2 = \frac{6A^2r_3-B^2r_4}{r_1}, r = \pm\frac{A^2-B^2}{4(A^4r_3-A^2B^2r_4)}, pq = 1$, then solution (13) becomes $I_1(\zeta) = g_0 + g_2(\pm\sqrt{-r}\mathrm{csch}(\sqrt{r}(\zeta)))^2$.
If $Y_4(\zeta) = I_5(\zeta), s = 1, g_0 = \frac{g_2r}{2s}, \nu = 0$, then $I_1(\zeta) = g_0 + g_2(\pm\sqrt{\frac{-r}{2}}\tanh(\sqrt{\frac{-r}{2}}(\zeta)))^2$.	If $g_0 = \frac{-A^2+(B^2\pm(A^2-B^2)}{2A^2r_1\epsilon}, g_2 = \frac{6A^2r_3-B^2r_4}{r_1}, r = \pm\frac{A^2-B^2}{2(A^4r_3-A^2B^2r_2)}, pq = 1$, then solution (16) becomes $I_5(\zeta) = g_0 + g_2(\pm\sqrt{\frac{-r}{2}}\tanh(\sqrt{\frac{-r}{2}}(\zeta)))^2$.
If $Y_5(\zeta) = I_6(\zeta), s = 1, g_0 = \frac{g_2r}{2s}, \nu = 0$, then $I_1(\zeta) = g_0 + g_2(\pm\sqrt{\frac{-r}{2}}\coth(\sqrt{\frac{-r}{2}}(\zeta)))^2$.	If $g_0 = \frac{-A^2+(B^2\pm(A^2-B^2)}{2A^2r_1\epsilon}, g_2 = \frac{6A^2r_3-B^2r_4}{r_1}, r = \pm\frac{A^2-B^2}{2(A^4r_3-A^2B^2r_2)}, pq = 1$, then solution (17) becomes $I_5(\zeta) = g_0 + g_2(\pm\sqrt{\frac{-r}{2}}\tanh(\sqrt{\frac{-r}{2}}(\zeta)))^2$.
If $Y_{10}(\zeta) = I_3(\zeta), s = 1, \nu = 0$, then $I_1(\zeta) = g_0 + g_2(\pm\sqrt{-r}\sec(\sqrt{r}(\zeta)))^2$.	If $g_0 = \frac{-A^2+(B^2\pm(A^2-B^2)}{2A^2r_1\epsilon}, g_2 = \frac{6A^2r_3-B^2r_4}{r_1}, r = \pm\frac{A^2-B^2}{4(A^4r_3-A^2B^2r_4)}, pq = 1$, then solution (14) becomes $I_3(\zeta) = g_0 + g_2(\pm\sqrt{-r}\sec(\sqrt{r}(\zeta)))^2$.
If $Y_{11}(\zeta) = I_4(\zeta), s = 1, \nu = 0$, then $I_2(\zeta) = g_0 + g_2(\pm\sqrt{r}\csc(\sqrt{r}(\zeta)))^2$.	If $g_0 = \frac{-A^2+(B^2\pm(A^2-B^2)}{2A^2r_1\epsilon}, g_2 = \frac{6A^2r_3-B^2r_4}{r_1}, r = \pm\frac{A^2-B^2}{4(A^4r_3-A^2B^2r_4)}, pq = 1$, then solution (15) becomes $I_4(\zeta) = g_0 + g_2(\pm\sqrt{-r}\csc(\sqrt{r}(\zeta)))^2$.
If $Y_3(\zeta) = (\pm\frac{4\delta_1\sqrt{r}}{(4\delta_1^2-s)\cosh(\sqrt{r}(\zeta+\zeta_0))\pm(4\delta_1^2+s)\sinh(\sqrt{r}(\zeta+\zeta_0))})^2g_2 + g_0$.	No corresponding solution found
If $Y_8(\zeta) = g_2(\pm\sqrt{-\frac{r}{2s}}(\frac{\pm\sqrt{D_1^2+D_2^2}-D_1\cosh(\sqrt{-2r}(\zeta+\nu))}{D_1\sinh(\sqrt{-2r}(\zeta+\nu))+D_2}))^2 + \frac{g_2r}{2s}$.	No corresponding solution found
If $Y_9(\zeta) = g_2(\pm\sqrt{-\frac{r}{2s}}(\frac{\cosh(\sqrt{-2r}(\zeta+\nu))}{\sinh(\sqrt{-2r}(\zeta+\nu))\pm i}))^2 + \frac{g_2r}{2s}$.	No corresponding solution found
If $Y_{16}(\zeta) = g_2(\pm\sqrt{\frac{r}{2s}}(\frac{\pm\sqrt{D_1^2-D_2^2}-D_1\cos(\sqrt{2r}(\zeta+\nu))}{D_1\sin(\sqrt{2r}(\zeta+\nu))+D_2}))^2 + \frac{g_2r}{2s}$.	No corresponding solution found
If $Y_{17}(\zeta) = +g_2(\pm\sqrt{\frac{r}{2s}}(\frac{\cos(\sqrt{2r}(\zeta+\nu))}{\sin(\sqrt{2r}(\zeta+\nu))\pm 1}))^2 + \frac{g_2r}{2s}$.	No corresponding solution found
If $Y_{18}(\zeta) = g_0 + g_2(\frac{4re^{\pm\sqrt{r}(\zeta+\nu)}}{e^{\pm 2\sqrt{r}(\zeta+\nu)}-4rs})^2$.	No corresponding solution found
If $Y_{21}(\zeta) = g_0 + g_2(\pm\frac{i}{\sqrt{-s}(\zeta+\nu)})^2$.	No corresponding solution found

Table 2. Comparison of methods: Advantages and limitations.

Method name	Advantages	Limitations
Modified Sardar Sub-Equation Method (MSSEM)	Yields diverse solutions: dark, bright, singular, periodic-singular, and combined solitons.	Solutions depend on constraint conditions. Not applicable to first-order equations.
Simplest Equation Method (SEM)	Derives multi-soliton solutions without altering the original NLPDE. Simple application without the need for bilinearization.	Limited to (1+1)-dimensional equations.
Bifurcation Analysis	Explains phase portraits, providing insights into the dynamical behavior of the system.	Applicable only to second-order equations.

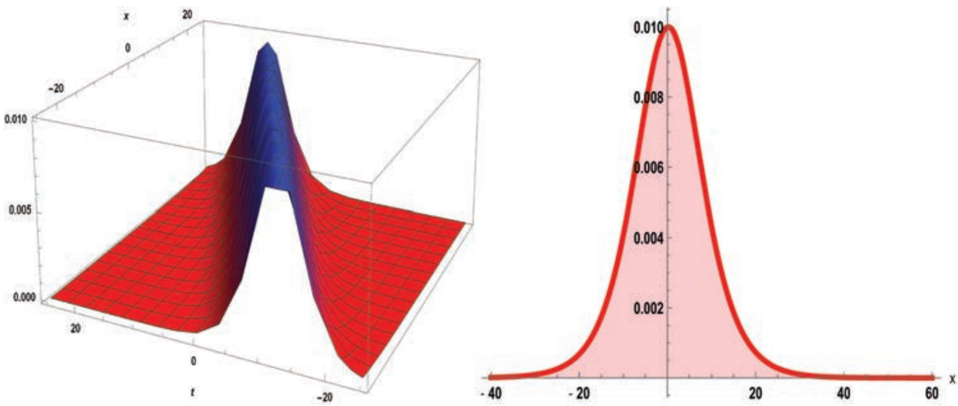

Fig. 2. (Color online) The evolution of one-soliton obtained from (15) for the parameter values via $c_1 = 0.4, g_2 = 1, k_1 = 0.2$.

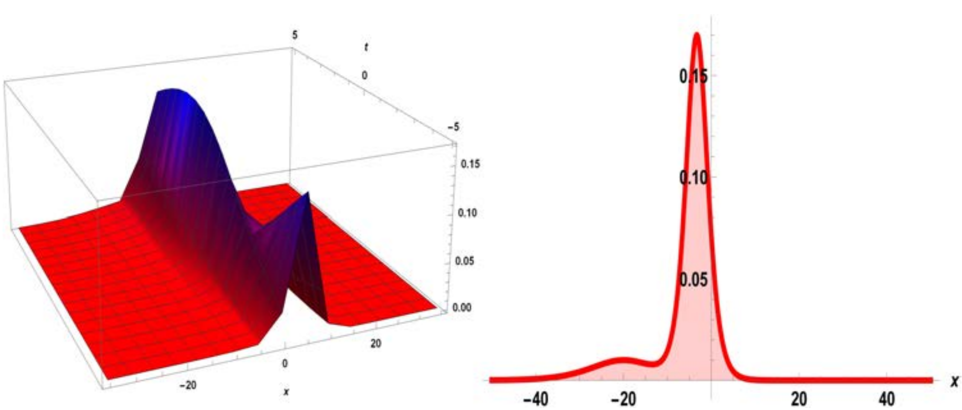

Fig. 3. (Color online) The evolution of two-soliton obtained from (16) for the parameter values $c_1 = 0.4,\ c_2 = 0.6,\ g_2 = 1,\ k_1 = 0.2$, and $k_2 = 0.8$.

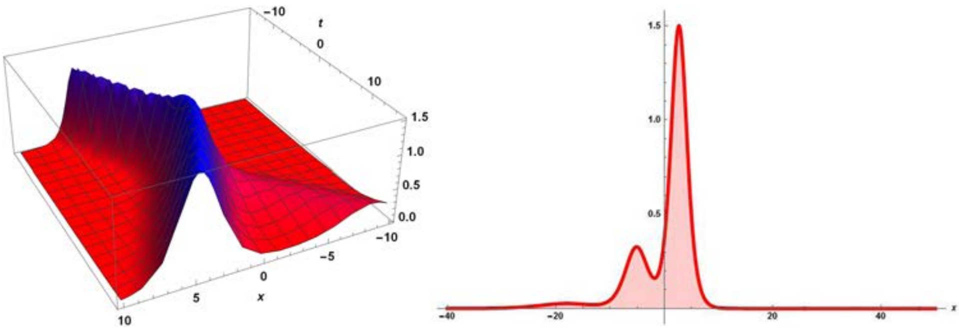

Fig. 4. (Color online) The evolution of three-soliton obtained from (17) for the parameter values $c_1 = 1,\ c_2 = 0.7,\ c_3 = 0.6,\ g_2 = 1.2,\ k_1 = 1,\ k_2 = 2$, and $k_3 = 0.3$.

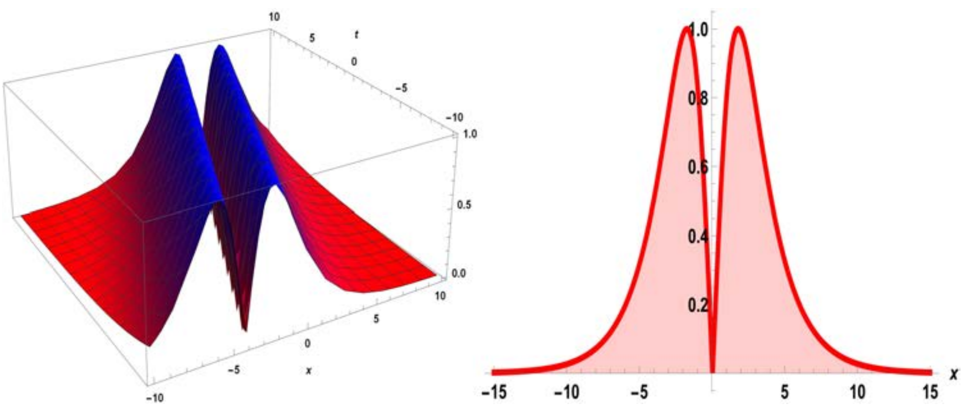

Fig. 5. (Color online) The evolution of dark–bright-soliton obtained from (25) for the parameter values $c = 0.5,\ g_0 = 1,\ g_2 = -3,\ k = 0.2, s = 0.75$, and $r = -0.5$.

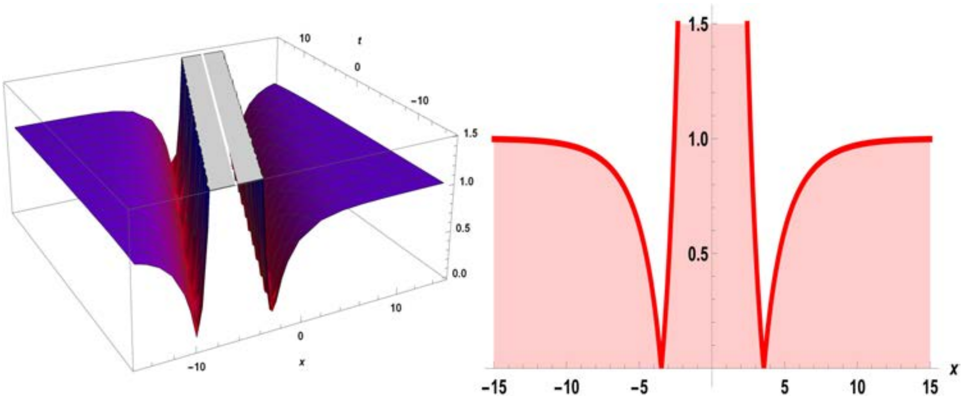

Fig. 6. (Color online) The evolution of dark-singular soliton obtained from (26) for the parameter values $c = 0.5,\ g_0 = 1,\ g_2 = -3,\ k = 0.2, s = 0.75$, and $r = -0.5$.

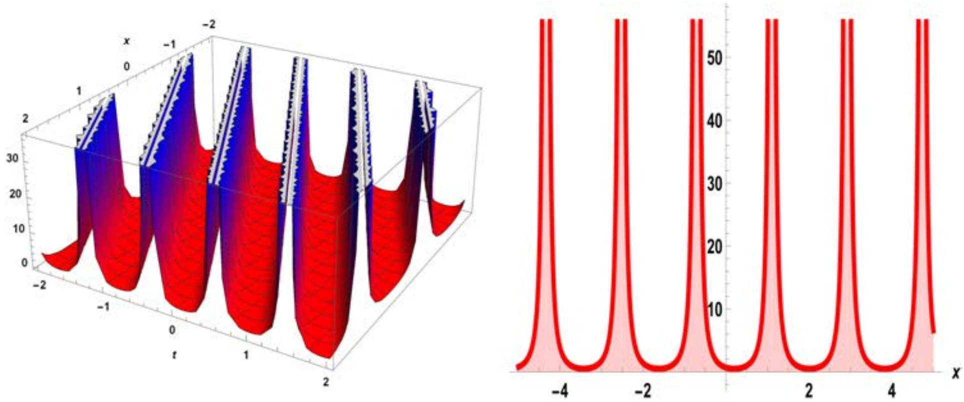

Fig. 7. (Color online) The evolution of periodic-singular soliton obtained from (29) for the parameter values $c = 2,\ g_0 = 1,\ g_2 = -1,\ k = 5,\ q = 0, s = 2$, and $r = -3$.

describe scenarios where the wave has periodic bursts of extreme intensity. Figure 8 indicates the singular soliton shape for $Y_{18}(\zeta)$. Singular solitons have infinite amplitude at specific points and highly localized energy spikes in the material. Physically, these have defects or sharp discontinuities within the crystal lattice.

Lastly, Figs. 9–11 exhibit phase portrait graphs for Eq. (42) obtained through bifurcation analysis for all possible cases. Bifurcation analysis in the terms of the strain wave equation gives valuable insights into the dynamic behavior of wave propagation in microcrystalline materials. By utilizing bifurcation analysis to the derived ODE, we can investigate how changes in system parameters influence the equilibrium states and stability of the wave system. This analysis helps us to identify different equilibrium points, such as center points, saddle points, and cusp points. For example, center points indicate stable periodic solutions while saddle points show regions of instability. Cusp points present critical transitions in the system's

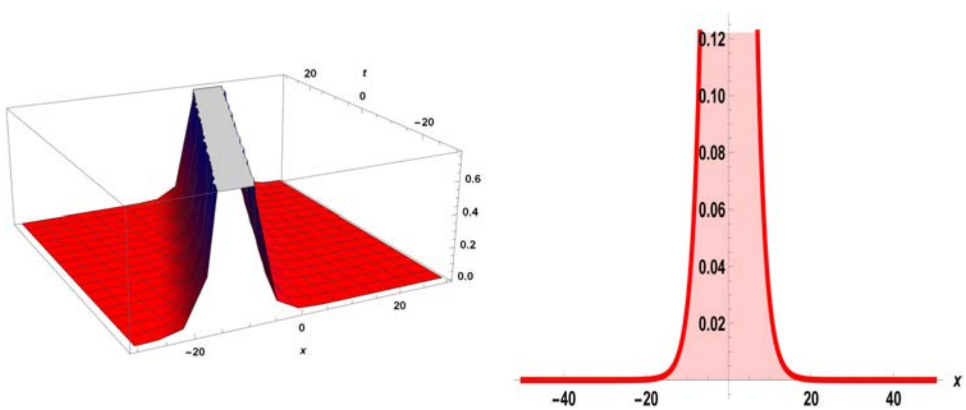

Fig. 8. (Color online) The evolution of singular soliton obtained from (37) for the parameter values $c = 2,\ g_0 = 1,\ g_2 = -1,\ k = 5,\ q = 0, s = 2$, and $r = 3$.

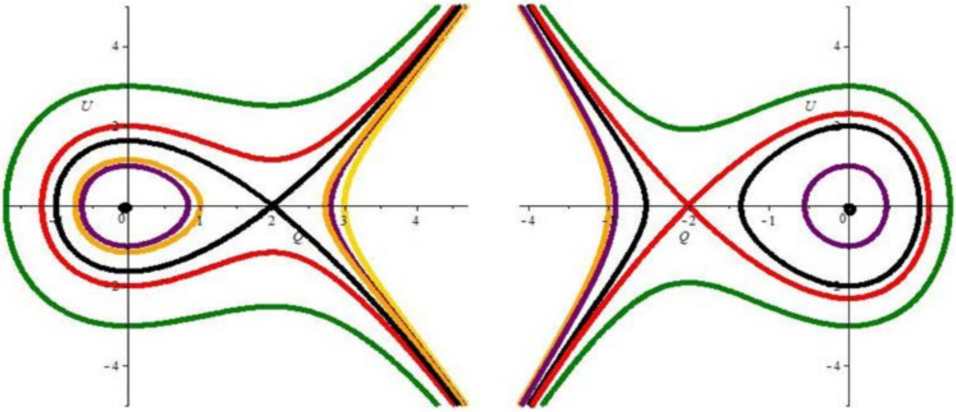

Fig. 9. (Color online) The phase portrait for (42) where (a) $b_1 > 0$ and (b) $b_1 0$.

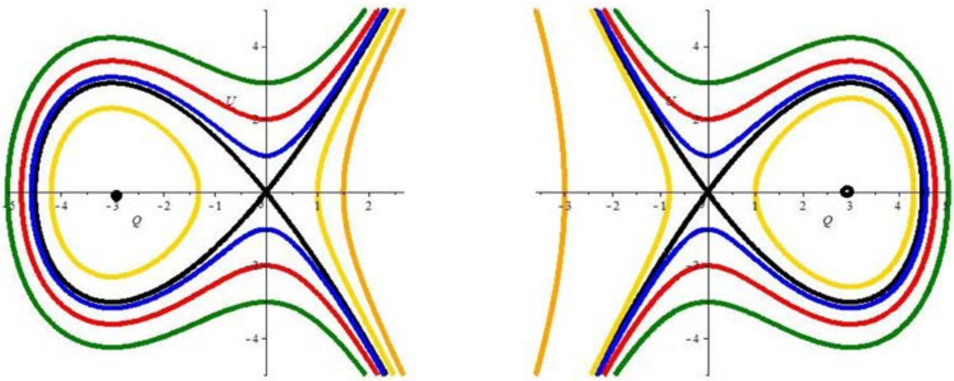

Fig. 10. (Color online) The phase portrait for (42) where (a) $b_1 > 0$ and (b) $b_1 0$.

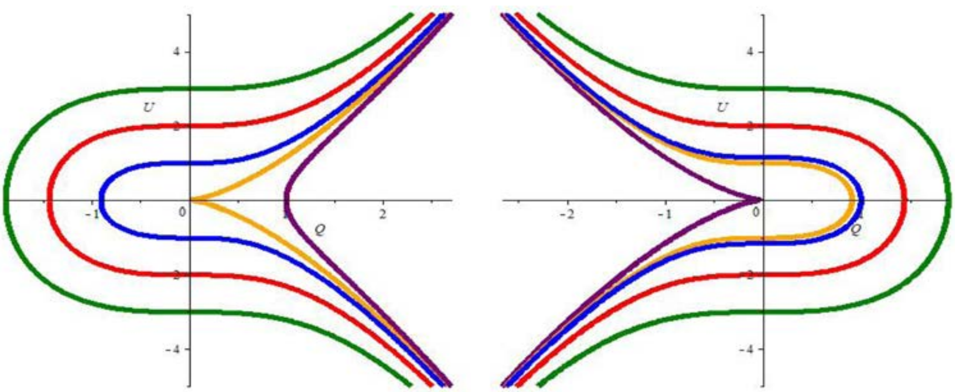

Fig. 11. (Color online) The phase portrait for (42) where (a) $b_1 > 0$ and (b) $b_1 0$.

dynamics to offer a understanding of how parameter changes affect the stability and propagation of strain waves.

6. Conclusion

This study has elucidated the intricate dynamics of wave propagation within microcrystalline materials through the utilization of advanced mathematical techniques and theoretical frameworks. By employing the strain wave equation and various solution methods such as the SEM and MSSEM, a comprehensive understanding of multi-soliton and other soliton solutions has been achieved. Furthermore, the application of dynamical system bifurcation theory has provided valuable insights into the phase diagrams governing the behavior of these materials. The significance of these findings extends beyond mere theoretical exploration, as they offer practical implications for understanding and manipulating wave phenomena in microstructured solids. Moreover, the physical dynamical representation of the obtained solutions through profile illustrations enriches our understanding of these complex systems, facilitating their interpretation and application in real-world scenarios.

Acknowledgment

All the authors are thankful to their respective institutes.

ORCID

Dean Chou https://orcid.org/0000-0001-9533-1918
Salah Mahmoud Boulaaras https://orcid.org/0000-0003-1308-2159
Hamood Ur Rehman https://orcid.org/0000-0003-3630-1705
Ifrah Iqbal https://orcid.org/0009-0004-6762-9580
Wen-Xiu Ma https://orcid.org/0000-0001-5309-1493

References

1. I. Iqbal, H. U. Rehman, M. Mirzazadeh and M. S. Hashemi, *Opt. Quantum Electron.* **55**(7) (2023) 588.
2. B.-L. Liang, Y. Wang, S.-H. Zhang, Q.-L. Guo, S.-F. Wang, G.-S. Fu, P. J. Simmonds and Z.-Q. Wang, *Phys. Lett. A* **381**(13) (2017) 1207.
3. S. Guo, A. R. Fritsch, C. Greenberg, I. B. Spielman and J. P. Zwolak, *Machine Learn.: Sci. Technol.* **2**(3) (2021) 035020.
4. A. Goswami, J. Singh, D. Kumar and Sushila, *Physica A: Statist. Mech. Appl.* **524** (2019) 563.
5. A. Goswami, Sushila, J. Singh and D. Kumar, *AIMS Math.* **5**(3) (2020) 2346.
6. A. Chen, F.-F. Wang and W. Zhang, *J. Phys. A: Math. Theor.* **43**(36) (2010) 365202.
7. E. Hesameddini and R. Gholampour, *Int. J. Math. Anal.* **4**(52) (2010) 2547.

8. H. C. Fogedby, *Phys. Rev. E* **57**(5) (1998) 4943.
9. E. M. Zayed and A.-G. Al-Nowehy, *Opt. Quantum Electron.* **49** (2017) 1.
10. N. Ahmed, M. Z. Baber, M. S. Iqbal, A. Annum, S. M. Ali, M. Ali, A. Akgül and S. M. El Din, *Sci. Rep.* **13**(1) (2023) 20033.
11. W. X. Ma, *Mathematics* **11**(22) (2023) 4664.
12. W. X. Ma, *Opt. Quantum Electron.* **52**(12) (2020) 511.
13. W. X. Ma, *Chaos Solitons Fractals* **180** (2024) 114539.
14. W. X. Ma, *Int. J. Geom. Methods Mod. Phys.* **20**(6) (2023) 2350098.
15. S. Kumar, A. Kumar and A.-M. Wazwaz, *Eur. Phys. J. Plus* **135**(11) (2020) 1.
16. A. R. Seadawy, M. Arshad and D. Lu, *Physica A: Statist. Mech. Appl.* **540** (2020) 123122.
17. G. Johari, S. Ram, G. Astl and E. Mayer, *J. Non-crystalline Solids* **116**(2–3) (1990) 2825.
18. A. J. Rossini, A. Zagdoun, F. Hegner, M. Schwarzwalder, D. Gajan, C. Copéret, A. Lesage and L. Emsley, *J. Amer. Chem. Soc.* **134**(40) (2012) 16899.
19. H. Struszczyk, *J. Appl. Polymer Sci.* **33**(1) (1987) 177.
20. R. M. Abdelhameed, S. F. Hammad, I. A. Abdallah, A. Bedair, M. Locatelli and F. R. Mansour, *J. Pharm. Biomed. Anal.* **235** (2023) 115609.
21. J. Leto and S. Choudhury, *Commun. Nonlinear Sci. Numer. Simul.* **14**(5) (2009) 1999.
22. H. Sun, Z. Zhang, Y. Liu, G. Chen, T. Li and M. Liao, *Adv. Quantum Technol.* **6**(11) (2023) 2300189.
23. H. ur Rehman, A. U. Awan, A. Habib, F. Gamaoun, E. M. T. El Din and A. M. Galal, *Res. Phys.* **39** (2022) 105755.
24. S. P. Joseph, *IOP SciNotes* **2**(1) (2021) 015002.
25. M. Moreno, R. Ambrosio, A. Torres, A. Torres, P. Rosales, A. Itzmoyotl and M. Domínguez, in *Crystalline Non-crystalline Solids*, published by InTech, Croatia, 2016, 147.
26. G. Ahmad, S. Mandal, A. Barua, T. Bhattacharyya and J. Roy, *J. Mater. Sci.: Mater. Electron.* **29** (2018) 11104.
27. Z. Ayati, K. Hosseini and M. Mirzazadeh, *Nonlinear Eng.* **6**(1) (2017) 25.
28. C. Cattani, T. A. Sulaiman, H. M. Baskonus and H. Bulut, *Opt. Quantum Electron.* **50** (2018) 1.
29. U. Asghar, M. I. Asjad, M. B. Riaz and T. Muhammad, *Res. Phys.* **58** (2024) 107550.
30. M. N. Alam, M. A. Akbar and S. T. Mohyud-Din, *Alexandria Eng. J.* **53**(1) (2014) 233.
31. M. Arshad, A. R. Seadawy, D.-C. Lu and A. Ali, *Commun. Theor. Phys.* **71**(10) (2019) 1155.
32. H. U. Rehman, N. Ullah and M. Imran, *Optik* **226** (2021) 165378.
33. A. Kurt, A. Tozar and O. Tasbozan, *J. Ocean Univ. China* **19** (2020) 772.
34. H. U. Rehman, M. S. Saleem, M. Zubair, S. Jafar and I. Latif, *Optik* **194** (2019) 163091.
35. X. Zeng and X. Yong, *Phys. Lett. A* **372**(44) (2008) 6602.
36. M. U. Shahzad, H. U. Rehman, A. U. Awan, Z. Zafar, A. M. Hassan and I. Iqbal, *Res. Phys.* **52** (2023) 106771.
37. H. U. Rehman, I. Iqbal, S. Subhi Aiadi, N. Mlaiki and M. S. Saleem, *Mathematics* **10**(18) (2022) 3377.
38. H. U. Rehman, N. Ullah and M. Imran, *Optik* **199** (2019) 163349.
39. S. Liu, Z. Fu, S. Liu and Q. Zhao, *Phys. Lett. A* **289**(1–2) (2001) 69.
40. H. U. Rehman, M. I. Asjad, I. Iqbal and A. Akgül, *Int. J. Appl. Nonlinear Sci.* **4**(1) (2023) 29.
41. M. I. Asjad, N. Ullah, H. U. Rehman and T. N. Gia, *Open Phys.* **19**(1) (2021) 770.
42. W. X. Ma and J.-H. Lee, *Chaos Solitons Fractals* **42**(3) (2009) 1356.
43. W. X. Ma, T. Huang and Y. Zhang, *Phys. Scr.* **82**(6) (2010) 065003.

44. A. Fahad, S. M. Boulaaras, H. U. Rehman, I. Iqbal and D. Chou, *Res. Phys.* **57** (2024) 107370.
45. S. Ibrahim, A. M. Ashir, Y. A. Sabawi and D. Baleanu, *Opt. Quantum Electron.* **55**(7) (2023) 617.
46. M. Mirzazadeh, Q. Zhou, E. Zerrad, M. F. Mahmood, A. Biswas and M. Belic, *Optoelectron. Adv. Mater. Rapid Commun.* **9**(11–12) (2015) 1342.
47. W. X. Ma and B. Fuchssteiner, *Int. J. Non-Linear Mech.* **31**(3) (1996) 329.